Finite Element Harmonic Modeling of Magnetoelectric Effect

Thu Trang Nguyen, Xavier Mininger, Frédéric Bouillault, and Laurent Daniel

Laboratoire de Génie Electrique de Paris, CNRS UMR8507, SUPELEC,
UPMC Univ Paris 6, Univ Paris-Sud, Gif-sur-Yvette, France

The magnetoelectric (ME) effect in composite materials results from the combination of the magnetostrictive effect and the piezoelectric effect via elastic interaction. This work focuses on the modeling of multilayer structures under dynamic excitation. The calculated ME coefficient versus frequency shows the enhancement of the ME effect at mechanical resonance in accordance with experimental measurements. The impact of electric conductivity is investigated. Applications on the ME sensor and tunable inductor are proposed.

Index Terms—**Finite element formulation, frequency effect, magnetoelectric effect, magnetostriction, piezoelectricity .**

I. Introduction

RESEARCH on magnetoelectric materials has increased rapidly in recent years due to many applications of such materials as magnetic sensors, memory devices, variable inductances [1]. The magnetoelectric phenomenon consists in the existence of a magnetization induced by an electric polarization, or conversely an electric polarization induced by a magnetization. Such a coupled property is characterized by ME coefficients. ME coefficients are larger in composite materials than in homogeneous materials [2]. Moreover, the enhancement of the ME coefficients at mechanical resonance frequencies [3] is useful for many smart devices. Therefore, the design and optimization for ME devices require accurate and compact numerical modeling.

Up to now, there are several numerical models: the frequency effect is integrated in the model of Liu *et al.* [4] but only from the mechanical point of view. The model of Galopin *et al.* [5] takes into account the nonlinear behavior of the magnetostrictive phase but only under quasi-static loadings.

The purpose of this work is to build a model based on the finite element method and accounting for the nonlinearity of magnetostriction and for the frequency effect (leading to eddy currents). In a first part, the formulation based on a thermodynamical approach is introduced. The model is then applied to a magnetoelectric sensor and a comparison to experimental data on a tunable inductor is proposed.

II. Equilibrium Equations

A. Mechanical Equilibrium

The mechanical equilibrium is given by

$$\mathrm{div}\mathbf{T} + \mathbf{f} = \rho_m \frac{\partial^2 \mathbf{u}}{\partial t^2} \tag{1}$$

where $\mathbf{T}$ is the stress tensor, $\mathbf{f}$ the driving force, $\mathbf{u}$ the displacement and ρ_m the mass density.

Manuscript received May 31, 2010; accepted September 13, 2010. Date of current version April 22, 2011. Corresponding author: T. T. Nguyen (e-mail: thutrang.nguyen@supelec.fr).

Color versions of one or more of the figures in this paper are available online at http://ieeexplore.ieee.org.

Digital Object Identifier 10.1109/TMAG.2010.2081356

B. Electromagnetic Equations

The electromagnetic equations are given by

$$\mathrm{curl}\mathbf{H} = \mathbf{J} + \frac{\partial \mathbf{D}}{\partial t} \tag{2}$$

$$\mathrm{div}\mathbf{D} = \rho \tag{3}$$

where $\mathbf{H}$ is the magnetic field, $\mathbf{J}$ the current density, $\mathbf{D}$ the electric induction, ρ the charge density $\rho = 0$.

III. Constitutive Laws

ME composite materials often consist in multilayers of piezoelectric (pz) and magnetostrictive (ms) materials.

A. Electroelastic Behavior

Considering that piezoelectric materials are usually prepolarized, the constitutive law is assumed to be linear around the polarization point

$$\begin{pmatrix} \widetilde{\mathbf{T}} \\ \widetilde{\mathbf{D}} \end{pmatrix} = \begin{bmatrix} \mathbb{c}_p & -\mathbb{e}_p^t \\ \mathbb{e}_p & \mathbb{c}_p \end{bmatrix} \begin{pmatrix} \widetilde{\mathbf{S}} \\ \widetilde{\mathbf{E}} \end{pmatrix} \tag{4}$$

where $\mathbf{S}$ is the strain tensor, $\mathbf{E}$ the electric field, $\mathbb{c}_p$ the stiffness tensor at constant electric field, $\mathbb{c}_p$ the electric permittivity at constant strain, and $\mathbb{e}_p$ the piezoelectric coefficients. We note $\widetilde{X}(\widetilde{a}, \widetilde{b})$ the small variation of X around a polarization point $X_0(a_0, b_0)$

$$\widetilde{X} = \frac{\partial X}{\partial a}(a_0, b_0)\widetilde{a} + \frac{\partial X}{\partial b}(a_0, b_0)\widetilde{b} \qquad X = X_0 + \widetilde{X}. \tag{5}$$

B. Magnetostrictive Behavior

1) General Form: Unlike the piezoelectric material, the magnetostrictive material is not prepolarized. Its constitutive law is strongly nonlinear and has to be accurately analyzed.

The total strain $\mathbf{S}$ is divided into the elastic strain $\mathbf{S}^e$ and the magnetostriction strain $\mathbf{S}^\mu$, $\mathbf{S} = \mathbf{S}^e + \mathbf{S}^\mu$ [6]. According to Hooke's law, the total stress is expressed by

$$t_{ij} = C^{ms}_{ijkl}\left(s_{kl} - s^\mu_{kl}\right) = C^{ms}_{ijkl}s_{kl} - t^\mu_{ij} \tag{6}$$

where C^{ms}_{ijkl} is the usual stiffness tensor of the magnetostrictive material under static loading. In the case of an isotropic material, (6) can be written using Lamé coefficients μ^* and λ^*

$$t_{ij} = 2\mu^*\left(s_{ij} - s^\mu_{ij}\right) + \delta_{ij}\lambda^*\left(s_{kk} - s^\mu_{kk}\right) \tag{7}$$

δ_{ij} is the Kronecker symbol ($\delta_{ij} = 1$ if $i = j$, 0 if $i \neq j$).

We assume that the magnetostriction phenomenon is isochoric and isotropic, and that the magnetostriction strain can

0018-9464/$26.00 © 2011 IEEE

be expressed as a parabolic function of the magnetic induction. We can then write [5]

$$s_{ij}^{\mu} = \frac{\beta}{2}(3b_i b_j - \delta_{ij} b_k b_k) \tag{8}$$

where β can be identified from experimental magnetostriction curves of the magnetostrictive material [7].

Using the thermodynamical approach of Besbes *et al.* [8] (writing $\partial t_{kl}/\partial b_i = \partial h_i/\partial s_{kl}$), taking s and b as independent variables, and noting ν_{ij} the reluctivity tensor of the magnetostrictive material, the magnetic field can be expressed

$$h_i = \nu_{ij} b_j - \frac{\partial t_{kl}^{\mu}}{\partial b_i}\left(s_{kl} - s_{kl}^{\mu}\right). \tag{9}$$

2) Linearized Form: In order to describe the constitutive law at a polarization point of the magnetostrictive material, the differentials of (6) and (9) are calculated, leading respectively to (10) and (11)

$$\widetilde{t}_{ij} = C_{ijkl}\widetilde{s}_{kl} - \frac{\partial t_{ij}^{\mu}}{\partial b_k}\widetilde{b}_k \tag{10}$$

$$\widetilde{h}_i = -\frac{\partial t_{kl}^{\mu}}{\partial b_i}\widetilde{s}_{kl} + \left[\nu_{ij} - \frac{\partial^2 t_{kl}^{\mu}}{\partial b_i \partial b_j}\left(s_{kl} - s_{kl}^{\mu}\right) + \frac{\partial t_{kl}^{\mu}}{\partial b_i}\frac{\partial s_{kl}^{\mu}}{\partial b_j}\right]\widetilde{b}_j. \tag{11}$$

As $s_{kk}^{\mu} = 0$ (isochoric magnetostriction), the term $\partial t_{kl}^{\mu}/\partial b_i$ can be calculated from (8) in the case of isotropic elasticity

$$\frac{\partial t_{kl}^{\mu}}{\partial b_i} = 2\mu^* \frac{\partial s_{kl}^{\mu}}{\partial b_i} = \mu^* \beta \frac{\partial(3b_k b_l - \delta_{kl} b_j b_j)}{\partial b_i} \tag{12}$$

where

$$\partial(3b_k b_l - \delta_{kl} b_j b_j)/\partial b_i = \begin{cases} 4b_i, & \text{if } k = l = i \\ -2b_i, & \text{if } k = l \neq i \\ 3b_l, & \text{if } k = i \neq l \\ 3b_k, & \text{if } l = i \neq k \\ 0, & \text{else.} \end{cases}$$

C. Specific Loading Conditions

In this part, we consider two specific cases associated to the applications presented in the last parts of the paper.

1) Polarization $\boldsymbol{B}_0 \neq 0$, $\boldsymbol{T}_0 = 0$: We obtain $(s_{ij} - s_{ij}^{\mu}) = 0$. Equations (10) and (11) become

$$\widetilde{t}_{ij} = C_{ijkl}\widetilde{s}_{kl} - \frac{\partial t_{ij}^{\mu}}{\partial b_k}\widetilde{b}_k \tag{13}$$

$$\widetilde{h}_i = -\frac{\partial t_{kl}^{\mu}}{\partial b_i}\widetilde{s}_{kl} + \left[\nu_{ij} + \frac{\partial t_{kl}^{\mu}}{\partial b_i}\frac{\partial s_{kl}^{\mu}}{\partial b_j}\right]\widetilde{b}_j. \tag{14}$$

These expressions (13) and (14) can be expressed in the form of system (16), introducing an effective reluctivity $\widetilde{\nu}^{\text{eff}}$ (15)

$$\widetilde{\nu}_{ij}^{\text{eff}} = \nu_{ij} + \frac{\partial t_{kl}^{\mu}}{\partial b_i}\frac{\partial s_{kl}^{\mu}}{\partial b_j} \tag{15}$$

$$\begin{pmatrix} \widetilde{\mathbf{T}} \\ \widetilde{\mathbf{H}} \end{pmatrix} = \begin{bmatrix} \widetilde{\mathbb{c}}_{\mu} & -\widetilde{\mathbb{q}}_{\mu}^{t} \\ -\widetilde{\mathbb{q}}_{\mu} & \widetilde{\nu}^{\text{eff}} \end{bmatrix} \begin{pmatrix} \widetilde{\mathbf{S}} \\ \widetilde{\mathbf{B}} \end{pmatrix} \tag{16}$$

2) Polarization $\boldsymbol{B}_0 = 0$, $\boldsymbol{T}_0 \neq 0$: From (12), we get $\partial t_{kl}^{\mu}/\partial b_i = 0$. Equations (10) and (11) can be simplified into

$$\widetilde{t}_{ij} = C_{ijkl}\widetilde{s}_{kl} \tag{17}$$

$$\widetilde{h}_i = \left(\nu_{ij} - \frac{\partial^2 t_{kl}^{\mu}}{\partial b_i \partial b_j} s_{kl}\right)\widetilde{b}_j. \tag{18}$$

We can also introduce an effective reluctivity $\widetilde{\nu}^{\text{eff}}$

$$\widetilde{\nu}_{ij}^{\text{eff}} = \nu_{ij} - \frac{\partial^2 t_{kl}^{\mu}}{\partial b_i \partial b_j} s_{kl} = \nu_{ij} - 4\beta\mu^*(3s_{ij} - \delta_{ij} s_{kk}). \tag{19}$$

From (17) and (18), the constitutive equation of the magnetostrictive material can be written

$$\begin{pmatrix} \widetilde{\mathbf{T}} \\ \widetilde{\mathbf{H}} \end{pmatrix} = \begin{bmatrix} \widetilde{\mathbb{c}}_{\mu} & \mathbb{0} \\ \mathbb{0} & \widetilde{\nu}^{\text{eff}} \end{bmatrix} \begin{pmatrix} \widetilde{\mathbf{S}} \\ \widetilde{\mathbf{B}} \end{pmatrix} \tag{20}$$

IV. Finite Element Formulation

In order to establish the 2-D finite element formulation, the Galerkin method is chosen with nodal element discretization.

A. Assumptions

1) Mechanical Assumption: The displacement $\mathbf{u}$ is chosen as mechanical variable in the finite element formulation

$$\mathbf{S} = \frac{1}{2}(\text{grad}\mathbf{u} + \text{grad}^t\mathbf{u}) = \mathcal{D}\mathbf{u}. \tag{21}$$

We consider a 2-D problem with plane stress assumption ($t_{31} = t_{32} = t_{33} = 0$) leading to the following relations:

$$\begin{cases} s_{31}^e = s_{32}^e = 0 \\ s_{33}^e = \frac{\lambda^*}{2\mu^* + \lambda^*}\left(s_{11}^e + s_{22}^e\right). \end{cases} \tag{22}$$

The displacement vectors in the working plane (from which the strain is defined) will be the unknown of the problem.

2) Electromagnetic Assumption: We consider a 2-D problem:

- The displacement currents are neglected in the Ampere's law. Only the conducting current is considered.
- No magnetic induction is considered in the direction perpendicular to the working plane (z-direction) and $\mathbf{B}$ is assumed to be invariant with z.
- The conservation of current along z-direction is written.

The electromagnetic equilibrium equations are written $\text{div}\mathbf{D} = 0$ and $\text{curl}\mathbf{H} = \mathbf{J}$ with $\mathbf{J} = 0$ in the nonconducting region.

From these assumptions, we deduce:

- The magnetic vector potential $\mathbf{a}$ is along z-direction and independent of z ($a_1 = a_2 = 0$).
- The electric field in the working plane $\mathbf{E}_{//}$ can be written: $\mathbf{E}_{//} = \text{grad}V$.
- The electric field in the conductor is along z-direction and can be calculated by: $e_3 = \partial(a_3 - a^0)/\partial t$ where a^0 is a constant with respect to x, y and z.
- We use $\mathbf{J} = \sigma\mathbf{E}$ where σ is the conductivity ($\sigma = 0$ in the piezoelectric material and $\sigma \neq 0$ in the magnetostrictive material). The conservation of current along z-direction is expressed by

$$\sigma \int_{\Delta} \frac{\partial(a_3 - a^0)}{\partial t} = 0 \tag{23}$$

where Δ is the total cross section of the conductor.

B. Finite Element Equation

1) Mechanical Formulation: From mechanical equilibrium (1) and the constitutive laws (4) and (16) or (20), noting Ω the

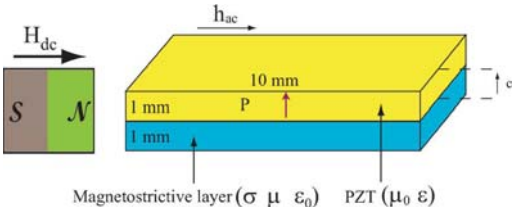

Fig. 1. Magnetoelectric bilayer.

study domain, Γ_s the boundaries of the study domain, the finite element formulation is

$$\int_\Omega [N]\left(\mathrm{div}(\mathbb{c}\mathbf{S}-\mathbb{e}\mathbf{E}-\mathbb{q}\mathbf{B})+\mathbf{f}-\rho_m\frac{\partial^2\mathbf{u}}{\partial t^2}\right)d\Omega=0 \quad (24)$$

where $[N]$ is the shape function. $\mathbb{q}=\mathbb{0}$ for the piezoelectric material, and $\mathbb{e}=\mathbb{0}$ for the magnetostrictive material. Using $U\mathrm{div}\mathbf{A}=\mathrm{div}U\mathbf{A}-\mathbf{A}\mathrm{grad}U$, (24) becomes

$$\begin{aligned}&\oint_{\Gamma_s}[N]\mathbb{c}\mathbf{S}d\Omega-\int_\Omega\mathbf{S}\mathbb{c}\,\mathrm{grad}[N]d\Omega-\oint_{\Gamma_s}[N]\mathbb{e}\mathbf{E}d\Omega+\\&\int_\Omega\mathbf{E}\mathbb{e}\,\mathrm{grad}[N]d\Omega-\oint_{\Gamma_s}[N]\mathbb{q}\mathbf{B}d\Omega+\\&\int_\Omega\mathbf{B}\mathbb{q}\,\mathrm{grad}[N]d\Omega+\rho_m\omega^2\int_\Omega[N]\mathbf{u}d\Omega=-\int_\Omega[N]\mathbf{f}d\Omega\end{aligned} \quad (25)$$

Imposing Dirichlet boundary conditions, (25) is simplified into

$$\begin{aligned}&-\int_\Omega\mathcal{D}\mathbf{u}\mathbb{c}\,\mathrm{grad}[N]d\Omega+\int_\Omega\mathrm{grad}V\mathbb{e}\,\mathrm{grad}[N]d\Omega\\&+\int_\Omega\mathrm{curl}\mathbf{a}\mathbb{q}\,\mathrm{grad}[N]d\Omega\\&+\rho_m\omega^2\int_\Omega[N]\mathbf{u}d\Omega=-\int_\Omega[N]\mathbf{f}d\Omega\end{aligned} \quad (26)$$

Equation (26) can be written in the matrix form

$$(\mathbb{K}_{uu}-\omega^2\mathbb{M})\mathbf{u}+\mathbb{K}_{up}V+\mathbb{K}_{ua}\mathbf{a}=\mathbf{f} \quad (27)$$

with

$$\begin{cases}\mathbb{K}_{uu}=\sum_e\int_{\Omega^e}\mathcal{D}[N]\mathbb{c}\mathcal{D}[N]d\Omega^e\\ \mathbb{K}_{up}=-\sum_e\int_{\Omega^e}\mathrm{grad}[N]\mathbb{e}\,\mathrm{grad}[N]d\Omega^e\\ \mathbb{K}_{ua}=-\sum_e\int_{\Omega^e}\mathrm{grad}[N]\mathbb{q}\,\mathrm{grad}[N]d\Omega^e\end{cases} \quad (28)$$

Ω^e is the partial domain. Equation (27) can be complemented with a damping term $\mathbb{D}\dfrac{\partial\mathbf{u}}{\partial t}=j\omega\alpha\mathbb{K}_{uu}\mathbf{u}$ with α the damping coefficient. Noting $\mathbb{K}^*_{uu}=\mathbb{K}_{uu}+j\omega\alpha\mathbb{K}_{uu}-\omega^2\mathbb{M}$ gives

$$\mathbb{K}^*_{uu}\mathbf{u}+\mathbb{K}_{up}V+\mathbb{K}_{ua}\mathbf{a}=\mathbf{f} \quad (29)$$

2) Electromagnetic Formulations: In a similar way, equations $\mathrm{div}\mathbf{D}=\rho$ and $\mathrm{curl}\mathbf{H}=\mathbf{J}$ gives these expressions

$$\mathbb{K}^t_{up}\mathbf{u}+\mathbb{K}_{pp}V=\rho \quad \text{and} \quad \mathbb{K}^t_{ua}\mathbf{u}+\mathbb{K}_{aa}\mathbf{a}=\mathbf{J} \quad (30)$$

with

$$\begin{cases}\mathbb{K}_{aa}=\sum_e\int_{\Omega^e}\mathrm{grad}[N]\tilde{\nu}^{\mathrm{eff}}\mathrm{grad}[N]d\Omega^e\\ \mathbb{K}_{pp}=\sum_e\int_{\Omega^e}\mathrm{grad}[N]\mathbb{c}\mathrm{grad}[N]d\Omega^e\end{cases} \quad (31)$$

The conservation of current along z-direction from (23) completes the finite element formulation

$$j\omega\sum_{e_\Delta}\int_{\Omega_e}a_3d\Omega^e-j\omega\Delta a^0=0. \quad (32)$$

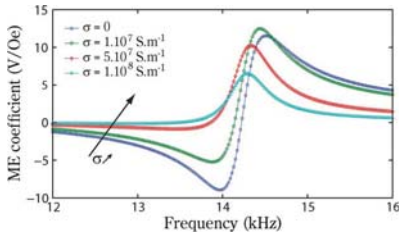

Fig. 2. ME voltage coefficient versus frequency for a bilayer (using a damping coefficient $\alpha=2\%$).

Finally, we obtain the system

$$\begin{bmatrix}\mathbb{K}^*_{uu}&\mathbb{K}_{up}&\mathbb{K}_{ua}&\mathbb{0}\\ \mathbb{K}_{pu}&\mathbb{K}_{pp}&\mathbb{0}&\mathbb{0}\\ \mathbb{K}_{au}&\mathbb{0}&\mathbb{K}_{aa}&\mathbb{J}^t\\ \mathbb{0}&\mathbb{0}&\mathbb{J}&\mathbb{S}\end{bmatrix}\begin{pmatrix}\mathbf{u}\\V\\\mathbf{a}\\a^0\end{pmatrix}=\begin{pmatrix}\mathbf{f}\\\rho\\\mathbf{J}\\\mathbf{0}\end{pmatrix} \quad (33)$$

where $\mathbb{K}_{pu}=\mathbb{K}^t_{up}$ describes the electro-mechanical coupling, $\mathbb{K}_{au}=\mathbb{K}^t_{ua}$ describes the magneto-mechanical coupling. The linear system (33) is solved using Gauss algorithm.

V. Magnetoelectric Sensor

A magnetoelectric bilayer is prepolarized by a static magnetic field H_{dc} under no applied stress. A harmonic magnetic field h_{ac} is applied, an electric voltage v_{ac} is obtained between the electrodes of the piezoelectric layer (PZT). This structure is presented in Fig. 1.

The prepolarization of the magnetostrictive material gives a constitutive law corresponding to (16). The magnetostrictive material parameters correspond to those of $CoFe_2O_4$ [9]. In order to investigate the effect of conductivity, four different values have been considered for σ. The ME coefficient defined as $\alpha=v_{ac}/h_{ac}$ is plotted in Fig. 2 as a function of the frequency. v_{ac} is the real part of V obtained from system (33), the imaginary part has similar resonance effect.

As shown in Fig. 2, the resonance is well captured by the model. This resonance effect has been reported by many researchers (e.g., Ncai *et al.* [10]). The resonance frequency is very close to the mechanical resonance frequency of the device ($f=14.5$ kHz). This frequency effect is strongly specimen dependent (sensor dimension, material parameters, etc). In absence of precise information, a quantitative comparison to published experimental results could not be performed. Concerning the effect of the conductivity, low conductivities leads to two peaks for the ME coefficient, the first one corresponding to the anti-resonance effect. The anti-resonance effect vanishes while conductivity increases. The higher the conductivity, the lower the electric voltage. This effect (due to the skin effect) is particularly sensitive for high frequencies. It has not been mentioned to our knowledge in earlier publications.

VI. Tunable Inductor

The trilayer shown in Fig. 3 is a tunable inductor which is described in [1]: Such electrostatically tunable magnetoelectric inductors have a large tunable range of up to 450%.

The thickness of each magnetostrictive layer (23 μm) is much less than that of the piezoelectric layer (500 μm). The modeling process is presented in Fig. 4.

The ME inductor is controlled by a static electric field $\pm E_{dc}$ between the electrodes of the piezoelectric layer. Using (20), for different points of polarization corresponding to different applied electric fields, the effective permeability is modified. Therefore, different inductances are obtained. The experimental

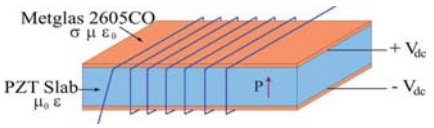

Fig. 3. Tunable magnetoelectric inductor.

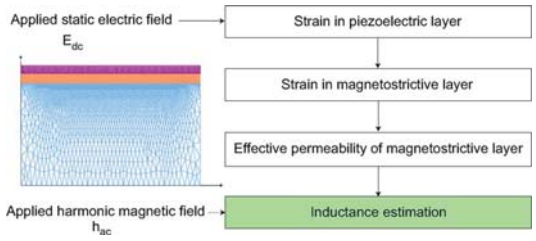

Fig. 4. Modeling procedure for the ME inductor, and mesh of a quarter of the inductor.

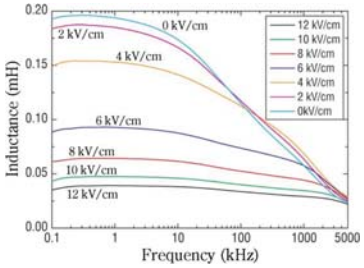

Fig. 5. Experimental results: Inductance versus frequency for different static electric fields E_{dc}.

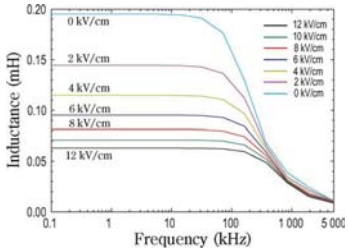

Fig. 6. Numerical results: Inductance versus frequency for different static electric fields E_{dc}.

results obtained by Lou *et al.* [1] are shown in Fig. 5. Fig. 6 shows the corresponding numerical results.

The inductances obtained by the model cannot be quantitatively compared to the experimental ones since some material parameters, such as β coefficient are unknown (β has been taken at 5.10^{-4} for the calculation, in order to fit the maximum inductance value at $E_{dc} = 0$). But experimental and numerical results have a very similar shape. The inductance decreases at high frequencies due to the skin effect. The tunability of the inductor is shown in Fig. 7, presenting the inductance value as a function of the applied electric field. An increase of the electric field causes an increase of the magnetostriction strain, and thus a decrease of the effective permeability due to the nonlinearity of magnetostriction as shown by equation (18). The maximum tunability can reach up to 250% in quasi-static regime.

VII. Conclusion

A 2-D finite element model has been built to investigate the harmonic ME effect. The piezoelectric behavior is defined using a linear constitutive law. A nonlinear constitutive law is used

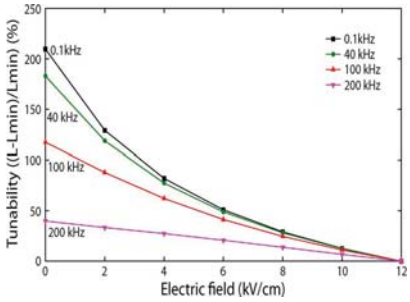

Fig. 7. Inductance versus applied electric field.

for the magnetostrictive material. A linearization procedure is proposed, allowing the definition of a linear constitutive law, depending on the polarization point and on the nonlinear constitutive law parameters.

The model is first implemented in the case of a magnetic field sensor. This case highlights the enhancement of ME coefficient for a resonance frequency, close to the mechanical resonance frequency. The second application concerns a tunable inductor. This smart device takes advantage of ME effect to control the inductance value. The model allows to capture this effect and reproduces the trends of experimental observations. A quantitative comparison would require a precise knowledge of specimen dimensions and material parameters. An experimental characterization to perform such a comparison is a work in progress. The development of a 3-D approach is also the object of current investigation.

Appendix
Proof of Equation (12)

From (6), the term t_{ij}^{μ} is written as

$$t_{ij}^{\mu} = C_{ijkl}^{ms} s_{kl}^{\mu} \tag{34}$$

In the case of isotropic material, using Lamé coefficients, this term is written [as in classical isotropic elasticity, see (7)]

$$t_{ij}^{\mu} = 2\mu^* s_{ij}^{\mu} + \delta_{ij}\lambda^* s_{kk}^{\mu} \tag{35}$$

Considering that the magnetostriction strain is isochoric, we have $s_{kk}^{\mu} = 0$ and therefore, (35) can be simplified into

$$t_{ij}^{\mu} = 2\mu^* s_{ij}^{\mu}. \tag{36}$$

Equation (12) is obtained by derivation of (36).

References

[1] J. Lou, D. Reed, M. Liu, and N. X. Sun, *Appl. Phys. Lett*, vol. 94, p. 112508, 2009.
[2] C. W. Nan, M. I. Bichurin, S. Dong, D. Veihland, and G. Srinivasan, *J. Appl. Phys.*, vol. 103, p. 031101, Feb. 2008.
[3] M. I. Bichurin, D. A. Filippov, V. M. Petrov, V. M. Laletsin, N. Paddubnaya, and G. Srinivasan, *Phys. Rev. B*, vol. 68, p. 132408, Oct. 2003.
[4] Y. X. Liu, J. G. Wan, J.-M. Liu, and C. W. Nan, *J. Appl. Phys.*, vol. 94, no. 8, pp. 5111–5117, Oct. 2003.
[5] N. Galopin, X. Mininger, F. Bouillault, and L. Daniel, *IEEE Trans. Magn.*, vol. 44, no. 6, pp. 834–837, Jun. 2008.
[6] L. Hirsinger and R. Billardon, *IEEE Trans. Magn.*, vol. 31, no. 3, pp. 1877–1880, May 1995.
[7] K. Azoum, M. Besbes, F. Bouillault, and T. Ueno, *Eur. Phys. J. Appl. Phys.*, vol. 36, no. 1, pp. 43–47, Oct. 2006.
[8] M. Besbes, Z. Ren, and A. Razek, *IEEE Trans. Magn.*, vol. 37, no. 1, pp. 3324–3328, Jan. 2001.
[9] J. Lee, J. G. Boyd, and D. C. Lagoudas, *Int. J. Eng. Sci.*, vol. 43, pp. 790–825, 2005.
[10] N. Cai, J. Zhai, C.-W. Nan, Y. Lin, and Z. Shi, *Phys. Rev. B*, vol. 68, p. 224103, 2003.